Applied Catalysis B: Environmental 166–167 (2015) 568–579

Contents lists available at ScienceDirect

Applied Catalysis B: Environmental

journal homepage: www.elsevier.com/locate/apcatb

# Impact of sulfur oxide on $NH_3$-SCR over Cu-SAPO-34

Kurnia Wijayanti[a], Stanislava Andonova[b], Ashok Kumar[b], Junhui Li[b], Krishna Kamasamudram[b], Neal W. Currier[b], Aleksey Yezerets[b], Louise Olsson[a,*]

[a] Competence Centre for Catalysis, Chemical Engineering, Chalmers University of Technology, SE-412 96 Gothenburg, Sweden
[b] Cummins Inc., 1900 McKinley Ave, MC 50183, Columbus, IN 47201, USA

ARTICLE INFO

*Article history:*
Received 24 July 2014
Received in revised form
16 November 2014
Accepted 19 November 2014
Available online 26 November 2014

*Keywords:*
Ammonia SCR
Cu-zeolites
SAPO-34
Deactivation
$SO_2$.

ABSTRACT

An investigation into the impact of sulfur oxide on the activity of Cu-SAPO-34 towards selective catalytic reduction of $NO_x$ by $NH_3$ has been conducted to clarify the possible mechanism of deactivation induced by sulfur. Several reactions including $NH_3$ storage/TPD, NO/$NH_3$ oxidations, standard and fast SCR, as well as SCR with an $NO_2/NO_x$ ratio of 75% were performed at temperature range of 150–500 °C over the fresh Cu-SAPO-34 after it had been sulfated at 300 °C with 30 ppm $SO_2$ in the presence of 8% $O_2$ and 5% $H_2O$ for 90 min. The catalyst is characterized by using XRD, BET, ICP-AES, $H_2$-TPR and micro-calorimetry. The BET surface area as well as the pore volume decreased after sulfur poisoning, hence some pores in the zeolite were blocked by sulfur. The standard SCR reaction was significantly influenced by the sulfur poisoning. The $H_2$-TPR data showed that there is less available copper that could undergo the redox cycle for the sulfated sample compared to the fresh sample and this could be the main reason for the deactivation seen. The conversion for $NO_x$ during standard SCR showed a more pronounced decrease in activity compared to that of fast SCR and the smallest effect of the sulfur poisoning was observed for SCR with the 75% $NO_2/NO_x$. Hence, the SCR reactions in the presence of $NO_2$ are less influenced by the sulfur on the surface and it is likely that the mechanism is different for SCR in the presence of $NO_2$. Cu-SAPO-34 produced very small amounts of $N_2O$ and its production correlated with the amount of $NO_2$ in the feed. From the calorimeter experiment, it was observed that the binding of $SO_2$ is very strong on the catalyst sites, most likely the copper sites, and the heat of adsorption of $SO_2$ was higher in the presence of $O_2$.


## 1. Introduction

Despite the substantial decrease in air pollutants, including $NO_x$, emitted during the past decades, the concentrations are still too high and need to be further reduced due to environmental and health issues. Particularly, in urban areas, transportation has proved to be the major source of $NO_x$ emission, and it is therefore critical to reduce it [1]. Ammonia-SCR, which has been used in stationary power plants, is considered the most efficient way of catalytically reducing $NO_x$ from vehicles operated in a lean environment. An aqueous solution of urea is injected into the hot exhaust, upstream of the SCR catalyst, producing ammonia via decomposition and hydrolysis. The ammonia formed is used as the reductant for $NO_x$ over an SCR catalyst [2,3]. The reaction is usually stoichiometric between $NH_3$ and NO producing $N_2$ and water according to the so-called 'standard SCR' reaction [4].

$$4NH_3 + 4NO + O_2 \rightarrow 4N_2 + 6H_2O \quad (1)$$

When equimolar NO and $NO_2$ are present, the rate of $NO_x$ reduction is higher, and the reaction follows the 'fast SCR' mechanism [5,6]:

$$4NH_3 + 2NO + 2NO_2 \rightarrow 4N_2 + 6H_2O \quad (2)$$

If $NO_2$ to NO ratio is greater than 1, the $NO_2$ would react via the '$NO_2$ SCR' step [5,6]:

$$8NH_3 + 6NO_2 \rightarrow 7N_2 + 6H_2O \quad (3)$$

Vanadia supported on titania with different promoters ($WO_3$ and $MoO_3$) were most commonly used for $NH_3$-SCR systems [2], especially for stationary plants. However, the instability of these catalysts at high temperatures, in combination with high toxicity, has led to the discovery of new catalysts, such as transition metals-exchanged zeolites that have been receiving a great deal of attention [7]. Copper and iron exchanged into narrow pore

* Corresponding author.
*E-mail address:* louise.olsson@chalmers.se (L. Olsson).

http://dx.doi.org/10.1016/j.apcatb.2014.11.043
0926-3373/

zeolites (ZSM-5, BEA, MOR, FER) have been investigated thoroughly and are showing promising results for $NO_x$ reduction [8–10]. Cu-zeolites offer a higher activity compared to Fe-zeolites at low temperatures and a sub-optimal $NO_2/NO_x$ ratio [11]. Unfortunately, these catalysts possess drawbacks such as a susceptibility towards hydrothermal conditions [12–15] besides hydrocarbon and chemical poisoning [16–19].

Considerable advancement was recently achieved when the Cu was exchanged into small-pore zeolites and silico-alumina phosphates with a chabazite (CHA) structure, such as Cu-SSZ-13, Cu-SAPO-34 and Cu-SSZ-39. These materials showed a remarkable hydrothermal stability compared to other types of zeolites [20–23]. It is generally accepted that dealumination is the major cause of structural damage and activity loss of large and narrow pore zeolites [8,15]. Since the dealumination product, an aluminum hydroxide moiety, ($Al(OH)_3$) has a larger diameter compared to that of the CHA structure, it is possible that the aluminum cannot escape from the pores or might be attached back to the framework maintaining the zeolite structures [20]. Another superiority of this class of catalysts is their durability towards hydrocarbon poisoning [16]. The large and medium pore zeolites adsorb significant amounts of hydrocarbons, particularly during cold-start conditions. This feature can results in detrimental effects, such as when the light-off temperature is reached and the stored hydrocarbon is suddenly oxidized, it may lead to a rising temperature that may destroy the zeolite. Again, the small-pore zeolites hinder this deactivation mechanism due to their limited diffusion of hydrocarbons [16,17,21].

In exhausts from vehicles, sulfur is always present due to residues in the fuel as well as those from lubricant oils. It is therefore crucial to examine the effect of sulfur on different components in the aftertreatment system. Several studies [24–32] have addressed the impact of sulfur poisoning in ammonia SCR systems. The vanadium-based catalysts were found to have a greater tolerance toward $SO_2$ poisoning than did the metal zeolite catalysts [24,27,28]. Among the zeolite-based catalysts, the impact of sulfur was more significant on Cu-zeolite than on Fe [24–26] and the adverse effect was most pronounced at low temperatures [25,27]. Unlike what was observed on Fe-zeolite and vanadia-based catalysts, the deactivation effects on Cu-zeolite due to $SO_2$ exposure can be minimized by maintaining the $NO_2$ fraction at 50% [24]. After regeneration by heating the poisoned catalysts at high temperatures under lean conditions, the $NO_x$ activity for both Fe and Cu-zeolite catalysts [26,29] was regained to the same level as before sulfation. However, Girard and co-workers [27] showed that the initial catalyst activity of copper zeolite could not be fully recovered if the catalyst had been exposed to high sulfur levels. The impact of sulfur on commercial Cu-SAPO-34 was examined by Zhang et al. [33]. They concluded that $SO_2$ inhibited the SCR activity at low temperature and was primarily due to the formation of ammonium sulfate species, but also by that sulfur blocks some site for $NO_x$. In a recent study by Kumar et al. [32], the effect of $SO_2$ and $SO_3$ on a small-pore Cu-zeolite SCR catalyst was studied. It was observed, that poisoning with $SO_3$ at 400 °C resulted in a more severe deactivation compared with using $SO_2$.

However, there are still several issues regarding the sulfur poisoning of Cu-SAPO-34 that are unclear. There are, to the best of our knowledge, no available studies that examine, for example, the effect of sulfur poisoning on fast and slow SCR, elemental and physical characterization of the sulfur poisoned Cu-SAPO-34 and the heat of adsorption of sulfur compounds during different conditions. These are points that are addressed in the present study. In more general terms, the objective of our study is to investigate the effects of $SO_2$ poisoning towards the activity of the Cu-SAPO-34 catalyst. The $NO_x$ reductions with different $NO_2$ fractions as well as the oxidation reactions are studied. Further, the adsorption–desorption behavior of the catalyst is examined using micro-calorimetry and TPD experiments. In addition, the fresh and sulfur poisoned catalyst are characterized with BET, ICP-AES and $H_2$-TPR.

## 2. Experimental methods

### 2.1. Catalyst preparation

#### 2.1.1. Zeolite synthesis

SAPO-34 used in this study was prepared using a hydrothermal synthesis method [34] during which 27.775 g of $H_3PO_4$ (85 wt%, Merck) was dissolved in 115.695 g of deionized water and stirred for 15 min at room temperature. 15.662 g psedoboehmite (74% $Al_2O_3$, PURAL SB-1, Sasol) was then slowly added during 2 h and the solution thereafter stirred for 12 h until a uniform gel had been obtained. Next, a homogenous solution of 18.435 g colloidal silica ($SiO_2$ 40 wt% in $H_2O$, LUDOX AS-40, Aldrich) and 21.105 g morpholine (tetrahydro-1,4-oxazine, Sigma-Aldrich) were slowly added for 1 h to the stirred P-containing solution. Following stirring for 7 h, the resulting mixture was then aged at ambient condition without stirring for 24 h. The solution was thereafter transferred and sealed into a 250 mL Teflon-lined stainless steel autoclave and heated in an oven at 200 °C for 72 h. After cooling to room temperature, the liquid phase was separated from the solid phase, which then was washed with deionized water several times and dried at 90 °C for 12 h. Finally, the powder obtained was calcined in air at 560 °C for 6 h with a ramping rate of 5 °C $min^{-1}$ in order to reach the desired temperature.

#### 2.1.2. Ion-exchange of zeolite

The ammonium form of SAPO-34 sample was prepared by exchanging the SAPO-34 with a 5.4 M solution of $NH_4NO_3$ (99%, Sigma Aldrich), using a ratio of volume of solution (mL) to weight of zeolite (g) of 7:1. The powder was slowly added to the agitated ammonium nitrate solution while the pH was maintained at around 3–3.5 by adding drops of diluted $NH_4OH$ solution. Following this procedure, the solution was heated to 80 °C and stirred continuously for 1 h, during which the pH was maintained in the interval of 3–3.5 using diluted $NH_4OH$. Thereafter, the mixture was cooled to room temperature and the solid separated. The solid was washed several times using milliQ water until the water used for washing was neutral in pH; the powder was thereafter dried in an oven at 90 °C for 12 h. The ammonium ion-exchange was carried out twice using the same procedure.

For copper ion exchange, a $Cu(NO_3)_2$ (98%, Alfa Aesar GmbH) 0.2 M solution was used with a volume (mL) ratio of solution to zeolite weight (g) of 4:1. The stirred solution was heated to 70 °C, and when this temperature had been reached, the powder was carefully added and the mixing maintained for 1 h before cooling to room temperature. After removing the liquid part, the resulting solid was washed several times with deionized water until neutral pH was received, dried for 12 h in an oven at 90 °C and finally calcined in air at 550 °C for 3 h with a ramping rate of 5 °C $min^{-1}$. The Cu-SAPO-34 powder obtained was then used for washcoating the monolith, catalyst characterization and micro-calorimeter experiments.

#### 2.1.3. Monolith preparation

The monolith was cut from a commercial honeycomb cordierite structure (20 mm in length, 21 mm in diameter, 400 cpsi) and then heated to 500 °C for 2 h. Initially, the monolith substrate was coated with a thin layer of alumina by immersing it several times in a mixture containing 95 wt% liquid phase (equal amount of ethanol and water) and 5 wt% solid phase of boehmite (Disperal D, Sasol, Gmbh) followed by drying in air for 2 min at 90 °C. Thereafter, the monolith was calcined at 500 °C for 2 h. This procedure was followed by catalyst impregnation using a slurry consisting of 20 wt% solid phase

and a liquid phase of ethanol and water (1:1). The Cu/SAPO-34 and boehmite ratio in the solid phase was 95:5 based on weight. Each time after dipping, the excess slurry was removed and the monolith dried in air for 2 min at 90 °C. The procedure was repeated several times until the desired amount of washcoat (~700 mg) was reached after which the monolith was calcined in air at 550 °C for 2 h.

### 2.2. Catalyst characterization

Elemental analysis of the Cu-SAPO-34 powder was measured using inductively coupled plasma sector field mass spectrometry (ICP-SFMS). The BET specific surface area and pore volume of the Cu-SAPO-34 powder were measured by $N_2$ physisorption at −195 °C using a Micromeritics ASAP 2010 instrument after degassing it at 210 °C for 3 h under vacuum conditions in order to remove adsorbed water. In addition, ICP-SFMS and BET surface area and pore volume were measured on crushed monoliths, before and after sulfur poisoning. The sulfur poisoned sample that were used in the characterization was the same monolith that had been used in the flow reactor experiments, thus after the sulfur poisoning the catalyst were used for multiple experiments. In order to verify the SAPO structure, X-ray diffraction (XRD) measurement of the powder was conducted using a "Scintag X2" diffractometer equipped with a computer-controlled goniometer and an X-ray source with Co Kα radiation (λ = 1.78897 Å), with scan run between 2$\theta$ of 5° and 40° at 0.02°/s.

The $H_2$-TPR (temperature-programmed desorption) set-up consisted of a vertical tube mounted in an electric furnace as a part of Setaram Sensys DSC (Digital Scanning Calorimeter), several mass flow controllers (MFC) as a gas mixing system and a Hiden HPR-20 QUI mass spectrometer (MS) for measuring the outlet gas concentration. During the measurements, the gas mixture (20 ml $min^{-1}$) was taken from a larger gas flow to improve the transient behavior of the gas mixing system. Approximately 100 mg of crushed monolith catalyst was placed on the sintered bed of the quartz tube and prior to the experiment the sample was pretreated with 8% $O_2$ in Ar at 500 °C for 20 min. The temperature was then decreased to 50 °C at which the sample was exposed to 3000 ppm of $H_2$ for 50 min followed by a temperature ramp of 10 °C $min^{-1}$ up to 800 °C. This procedure was performed for the fresh catalyst as well as the sulfated one. For the fresh sample before the oxygen pretreatment, the catalyst was degreened by exposing it to 400 ppm $NH_3$, 400 ppm NO, and 8% $O_2$ in Ar at 700 °C for 2 h.

### 2.3. Micro-calorimeter experiments

The micro-calorimetric measurement was performed using the same set-up used for the $H_2$-TPR experiment. Two quartz tubes were mounted inside the DSC, one where the catalyst powder was placed on a sintered plate, while the other was used as a reference. Argon was used as an inert balance for all experiments and prior to each measurement, the surface of the catalyst was cleaned by exposing it to 8% $O_2$ at 500 °C for 20 min.

The following experiments were carried out using the calorimeter system:

a. $SO_2$ storage
   These experiments were conducted in order to measure the heat of adsorption of $SO_2$ on Cu-SAPO-34 at different temperatures. 100 mg of the catalyst powder was exposed to 100 ppm $SO_2$ at 300 °C for 120 min followed by Ar only for 90 min before the temperature was ramped to 800 °C, with a ramp rate of 10 °C $min^{-1}$. In the next experiment, 8% oxygen was added to the $SO_2$ during the adsorption period in order to investigate its influence on the $SO_2$ adsorption. Using the same procedure, the experiments with and without oxygen were repeated at an adsorption temperature of 500 °C. For each of the above-discussed experiment, new powder samples were used.
b. $NH_3$ stepwise experiments
   For these experiments the powder was first degreened at 700 °C for 2 h using 400 ppm NO, 400 ppm $NH_3$ and 8% $O_2$. After the degreening and above described pretreatment, Cu-SAPO-34 powder was exposed to 500 ppm $NH_3$ at 500 °C for 3 h, followed by cooling in Ar only to 450 °C and the sample was again exposed to 500 ppm $NH_3$ for 3 h. The procedure was then repeated at lower temperatures with step of 50 °C to the lowest one of 50 °C (400, 350, 300, etc.), with the exception that at 50 °C, the period of $NH_3$ exposure was 4 h. In order to test the reproducibility, the experiment was repeated using similar protocol, however in the last experiment, the $NH_3$ adsorption at 450 °C was excluded. The ammonia exposure at the highest temperature (500 °C) was not used in order to determine the heat of adsorption but instead to clean the surface from possible remaining oxygen left from the pretreatment. In addition, the adsorbed amount of ammonia at the highest temperatures (450 and 500 °C) were small, resulting in that the heat produced did not reach a stable level and therefore the results at 450 °C could not be used.

### 2.4. Activity measurements in the flow reactor system

Activity tests of Cu-SAPO-34 catalysts were carried out in a flow reactor system. The monolith catalyst (20 mm in length, 21 mm in diameter, 400 cpsi) was placed in a quartz tube, which was 800 mm in length and 22 mm in inner diameter. The monolith was wrapped in quartz wool to ensure that there was no gas slip around the sample. The inlet gas feed was regulated using several Bronkhorst mass flow controllers. The steam was produced by an evaporator and mixing system (Bronkhorst CEM system) and then fed to the reactor. Two thermocouples were inserted into the monolith, one for measuring gas temperature positioned 10 mm before the catalyst and the other placed inside a centre channel showing the catalyst temperature. The outlet gases from the reactor were analyzed by an MKS Multigas 2030 FTIR spectrometer, which monitored the concentration of $NH_3$, NO, $NO_2$, $N_2O$, as well as $H_2O$. The total flow of 3500 ml $min^{-1}$, resulting in 30,300 $h^{-1}$ GHSV, was used and argon was chosen as the inert balance in all experimental sequences.

In order to obtain a stable catalytic behavior during measurements, the catalyst was first degreened by being conditioned with 400 ppm $NH_3$ + 400 ppm NO + 8% $O_2$ + 5% $H_2O$ in Ar at 700 °C for 120 min. Prior to each experimental sequence, the catalyst was pretreated at 500 °C using 8% $O_2$ + 5% $H_2O$ for 20 min to clean its surface. The effects of $SO_2$ poisoning were investigated by measuring the $NH_3$ storage/release (temperature-programmed desorption, TPD) and several activity measurements for fresh catalyst and catalyst after each $SO_2$ exposure. Sulfation treatment at 300 °C using 30 ppm $SO_2$ for 90 min in the presence of 8% $O_2$ and 5% $H_2O$ was carried out twice and after each treatment, the catalyst activity was tested during five repeated standard SCR experiments in order to reach stable activity. This sequence was followed by fast SCR, NO oxidation, $NH_3$ oxidation, $NH_3$ storage/TPD and $NO_2$ SCR. A detailed sequence of experiments is listed in Table 1. It should be noted that all experiments were made on the same monolith, with sequential poisoning.

The experiments performed over fresh and sulfated catalyst are described below:

a. Ammonia storage and temperature-programmed desorption (TPD) experiment:
   First, the catalyst was exposed to 400 ppm $NH_3$ + 5% $H_2O$ at 150 °C for 40 min, followed by 5% $H_2O$ in Ar for 30 min. The

**Table 1**
Experimental sequence performed in the flow reactor system.

| Sample | Experiment | Acronym of the experiment |
|---|---|---|
| Fresh | $NH_3$ storage and TPD | Fresh |
| | Standard SCR | Fresh |
| | Fast SCR | Fresh |
| | NO oxidation | Fresh |
| | $NH_3$ oxidation | Fresh |
| | Slow $NO_2$ SCR | Fresh |
| After 1st $SO_2$ poisoning | Standard SCR (5 times) | $SO_2$-1A to 1E |
| | Fast SCR | $SO_2$-1F |
| | NO oxidation | $SO_2$-1G |
| | $NH_3$ oxidation | $SO_2$-1H |
| | $NH_3$ storage and TPD | $SO_2$-1I |
| | Slow $NO_2$ SCR | $SO_2$-1J |
| After 2nd $SO_2$ poisoning | Standard SCR (5 times) | $SO_2$-2A to 2E |
| | Fast SCR | $SO_2$-2F |
| | NO oxidation | $SO_2$-2G |
| | $NH_3$ oxidation | $SO_2$-2H |
| | $NH_3$ storage and TPD | $SO_2$-2I |
| | Slow $NO_2$ SCR | $SO_2$-2J |

temperature was then increased to 500 °C, with a ramp rate of 10 °C $min^{-1}$.

b. Activity measurements

The reaction studies including standard, fast and $NO_2$ SCR, as well as NO and $NH_3$ oxidation were carried out at 150, 200, 250, 300, 400 and 500 °C. The activity for NO and ammonia oxidation was examined by exposing the catalyst to 400 ppm NO or $NH_3$ + 8% $O_2$ + 5% $H_2O$ by increasing the temperature stepwise from 150 to 500 °C, with a ramp rate of 20 °C $min^{-1}$ between the temperature steps. The same procedure was used for the SCR reactions using 400 ppm $NH_3$, 400 ppm $NO_x$, 8% $O_2$ and 5% $H_2O$, with $NO_2$ to $NO_x$ ratio of 0, 50 and 75%.

## 3. Results and discussion

### 3.1. Catalyst characterization

#### 3.1.1. XRD, ICP and BET surface area

The XRD analysis was conducted for SAPO-34, Cu-SAPO-34 and a commercial SAPO-34 from Green Stone Swiss Co., Ltd. as shown in Fig. 1. The results clearly showed that the CHA framework was maintained in the Cu-SAPO-34 despite the low pH of the ion exchange process.

An ICP-SFMS analysis of Cu-SAPO-34 powder was performed to gather information of the Cu, Si, Al and P contents of the catalyst powder sample before washcoating, as well as examining if there were any impurities. This measurement resulted in 1 wt% Cu, 12.7 wt% $SiO_2$, 35.2 wt% $Al_2O_3$ and 29.9 wt% $P_2O_5$. $Fe_2O_3$ and $Na_2O$ were below the detection limit, which is 0.1 wt% for $Fe_2O_3$ and 0.05 wt% for $Na_2O$. The Cu ion-exchange level was 0.12, based on the Cu to Si ratio, showing that the copper was under-exchanged. The BET surface area and pore volume were determined to be 595 $m^2$ $g^{-1}$ and 0.28 $cm^3$ $g^{-1}$, respectively.

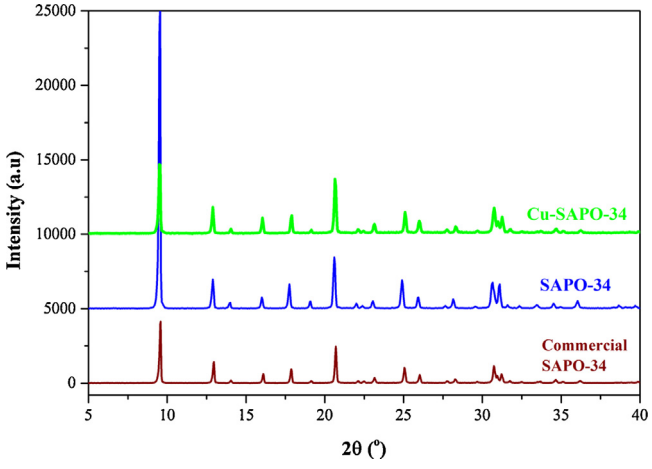


**Fig. 1.** XRD pattern for Cu-SAPO-34, SAPO-34 and commercial SAPO-34 samples.

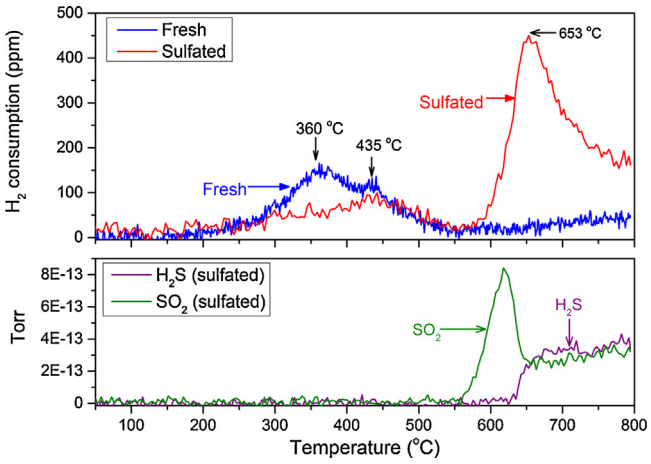


**Fig. 2.** $H_2$-TPR of fresh and sulfated crushed monolith of Cu-SAPO-34.

In addition, an analysis was also made of the sulfur-poisoned monolith and for a fresh monolith to examine the impact of the sulfur poisoning (see Table 2). The amount of sulfur was significantly higher for the poisoned sample, showing that sulfur was still remaining in the sample after repeated experiments to 500 °C. The small amount of sulfur observed in the fresh catalyst was likely attributed to either measuring accuracy of the method or owing to the cordierite, since no sulfur-containing precursor was used during the synthesis. On a molar base, there is about 0.3 mol S per Cu atom. Thus, it is possible that all sulfur is attached to copper atoms. The presence of sulfur also blocks some channels, which was observed by the decrease in the BET surface area, as well as the pore volume (Table 2).

#### 3.1.2. $H_2$-TPR

The redox properties of the fresh and sulfated Cu-SAPO-34 were studied by conducting TPR analysis and measuring the outlet $H_2$ concentration during the temperature ramp from 50 up to 800 °C. The $H_2$ consumption as a function of temperature during the $H_2$-TPR experiment presented in Fig. 2 shows that a prominent peak of the fresh sample appeared at around 360 °C. The UV–vis measurement on similar Cu-SAPO-34 (data are not shown here) indicated the copper in samples with low copper loading is mostly in the form of copper hydroxyls, thus in $Cu^{2+}$ form [35]. Moreover, calculation of the $H_2$ consumption of the main peak (up to 550 °C) resulted in $H_2$/Cu ratio of 0.67, which means that not all copper species is reduced to $Cu^0$. This is supported by the total integration of the curve, which resulted in the molar ratio of $H_2$ to Cu of 0.86, which showed that the reduction was incomplete even up to 800 °C. Another peak was observed for the fresh sample at 435 °C, even though it was relatively small compared to the one at 360 °C. Xue et al. [36] also reported that some copper in Cu-SAPO-34 was difficult to reduce and they detected a $H_2$ consumption peak as high as 837 °C for a sample containing 0.98 wt% Cu. The coexistence of different copper species in the Cu-SAPO-34 is in accordance with recent study by Gao et al. [37]. In addition, Xue et al. [36] found three different peaks in Cu-SAPO-34 and proposed that the first peak originated from reduction $Cu^{2+}$ to $Cu^+$, the second one was

**Table 2**
Characterization of fresh and sulfated Cu-SAPO-34.

| Monolith sample | S content (wt%) | $S_{BET}$ ($m^2$/(g monolith)) | $V_p$ ($cm^3$/(g monolith)) | $S_{BET}$ ($m^2$/(g wash-coat))* | $V_p$ ($cm^3$/(g washcoat))[a] |
|---|---|---|---|---|---|
| Fresh Cu-SAPO-34 | 0.027 | 113 | 0.07 | 431 | 0.27 |
| Sulfated Cu-SAPO-34 | 0.114 | 89 | 0.06 | 318 | 0.21 |

[a] Estimated based on washcoat amount.

ascribed to reduction nanosize CuO crystallites and the last peak was the $Cu^+$ to $Cu^0$. In this study, we interpret the main peak as the reduction $Cu^{2+}$ to $Cu^+$ and possibly also by the reduction of $Cu^+$ to $Cu^0$, as proposed by Leistner and Olsson [35]. The smaller peak could be attributed to $Cu^+$ to $Cu^0$ or by the presence of small amounts of CuO as observed by Gao et al. [37].

A broad peak was noticeable after the catalyst treated with $SO_2$ at the same temperature range as the fresh sample, which might be attributed to the reduction of $Cu^{2+}$ to $Cu^+$ and $Cu^+$ to $Cu^0$. Further, the peak was much lower with calculated $H_2$/Cu ratio of 0.51, which is due to the blocking effect of sulfur on the copper sites. A huge $H_2$ consumption peak was seen at temperature of 653 °C, while $SO_2$ and $H_2S$ production was also detected from the MS measurement as demonstrated by Fig. 2. It is likely that $H_2$ is consumed by reacting with sulfates or other surface $SO_2$ groups, which are formed during sulfur treatment, to produce $SO_2$ and $H_2S$. $SO_2$ signals perceived further supports that sulfur is mainly stored as either sulfates or surface $SO_2$ groups which were also suggested by Zhang et al. [33] using DRIFT spectroscopy.

### 3.2. Micro-calorimeter measurements

Micro-calorimetry is a powerful technique for measuring the heat of adsorption on the surface. Wilken et al. [38] developed a method for detecting the coverage-dependent heat of adsorption at atmospheric pressure and applied this method to ammonia adsorption on Cu-BEA. Ammonia was first introduced over the catalyst at high temperature (500 °C), resulting in only the most strongly bound ammonia being adsorbed, producing a high $\Delta H$. Thereafter, the temperature was decreased, while exposing the catalyst to Ar alone and at 400 °C, ammonia is again added, now resulting in a lower $\Delta H$ because more loosely bound ammonia was adsorbed. This procedure was repeated several times while lowering the temperature [38]. In our present study, we applied this technique of ammonia adsorption on Cu-SAPO-34, conducting the adsorption at 500, 450, 400, 350, etc. down to 50 °C. The resulting heat of adsorption versus adsorption temperature is shown in Fig. 3. The ammonia exposure at the highest temperatures (500 °C) was not used in order to determine the heat of adsorption but instead to clean the surface from the possible remaining oxygen left from the pretreatment. In addition, at 450 °C the adsorption was small, resulting in that stable heat flow was not received, which influence the accuracy of the measurement and therefore the results from 450 °C was not used. From 300 to 50 °C, the same trend as for Cu-BEA [38] was observed for Cu-SAPO-34 with decreasing $\Delta H$ when decreasing the temperature because of more loosely bound ammonia. However, the binding strength of ammonia to Cu-SAPO-34 was higher compared to that of Cu-BEA, for example at 300 °C, $\Delta H$ for ammonia on Cu-SAPO-34 was 137 kJ/mol, while on Cu-BEA only 94 kJ/mol was obtained. The differences were smaller using 100 °C as adsorption temperature, with 86 kJ/mol for Cu-SAPO-34 and 75 kJ/mol for Cu-BEA [38]. The heat of adsorption for ammonia on Cu-SAPO-34 was also higher than on Cu-ZSM-5 (104.8 kJ/mol) [39] and H-ZSM-5 (114 kJ/mol) [40]. Surprisingly, the heat of adsorption at 400, 350 and 300 °C were similar. One reason for this behavior could be that after the ammonia is turned off at 400 and 350 °C, more than half of the ammonia adsorbed was desorbed again. Thus, significant amount of the ammonia adsorbed at 400 °C is readsorbed at 350 and 300 °C again. The ammonia adsorption experiment was repeated to examine the reproducibility of the procedure. Referring to the first experiment where the heat of adsorption at 450 °C were difficult to measure, for the repeated experiment the heat of adsorption measurement was then conducted from 500, 400, 350, 300, etc. down to 50 °C. As in the previous experiment, the adsorption at 500 °C was used to remove possible oxygen left on the sites from the pre-treatment. Result from the repeating experiment shows an excellent reproducibility as presented in Fig. 3.

The heat of adsorption of $SO_2$ and $SO_2 + O_2$ over Cu-SAPO-34 was measured at 300 and 500 °C, respectively, with the results shown in Fig. 4. The heat of adsorption was high for $SO_2$, e.g. 229 kJ/mol at 300 °C, which shows that the sulfur species formed are binding very strongly to the catalyst sites. The $\Delta H$ was higher when increasing the adsorption temperature to 500 °C, which was in line with earlier DSC measurements with ammonia [38], where more loosely bound species were also present at lower adsorption temperatures.

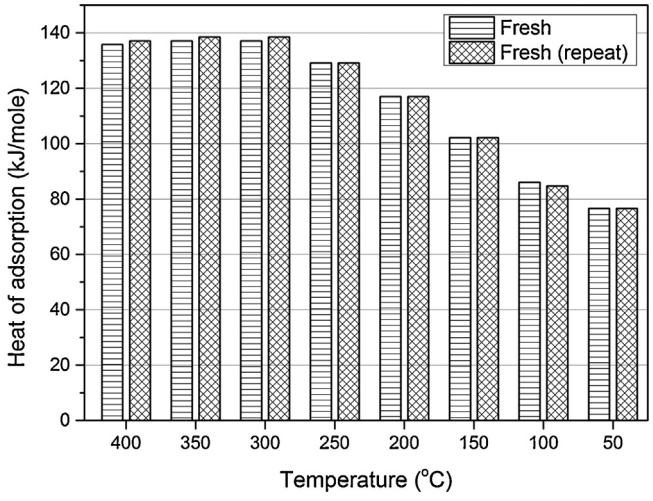


**Fig. 3.** Heat of adsorption of $NH_3$ at various levels of temperature in fresh Cu-SAPO-34.

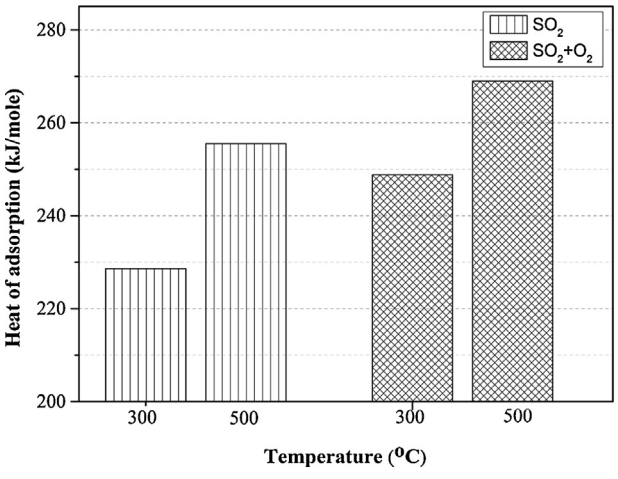


**Fig. 4.** Heat of adsorption of $SO_2$ over Cu-SAPO-34. The catalyst was exposed to 100 ppm $SO_2$ at 300 and 500 °C with and without 8% $O_2$.

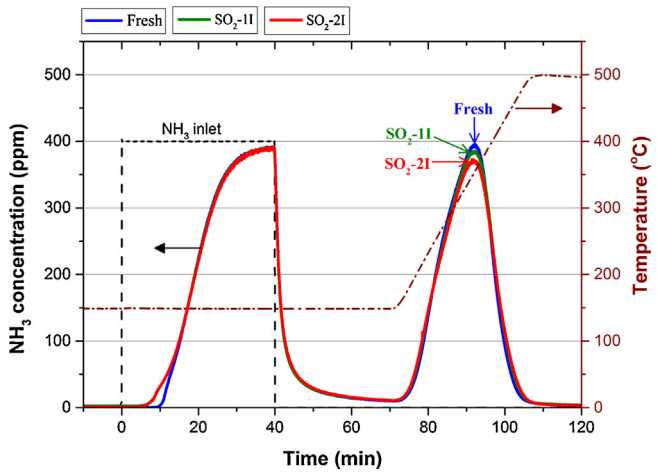


**Fig. 5.** $NH_3$ concentration during $NH_3$ storage (150 °C) and TPD (150–500 °C) over fresh and sulfur-treated ($SO_2$-1I and $SO_2$-2I) Cu-SAPO-34. The catalyst was exposed to 400 ppm $NH_3$ + 8% $O_2$ + 5% $H_2O$ in Ar during adsorption period.

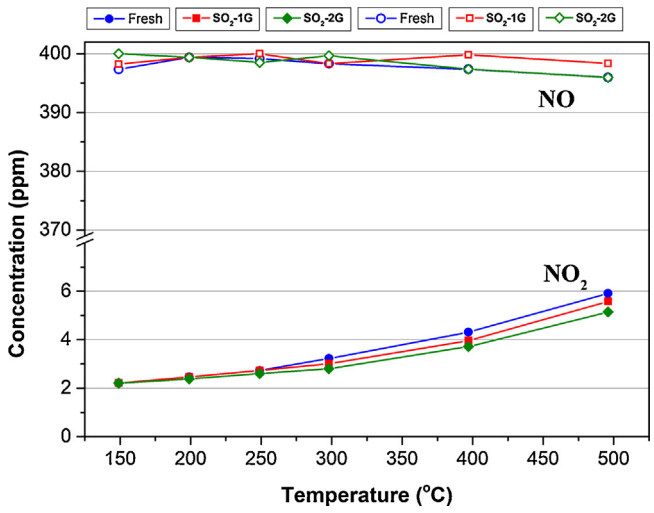


**Fig. 6.** Steady-state NO and $NO_2$ concentration during NO oxidation over fresh and sulfated Cu-SAPO-34 from 150 to 500 °C. The catalyst was exposed to 400 ppm NO + 8% $O_2$ + 5% $H_2O$ in Ar. The experimental notation is presented in Table 1.

Another interesting feature was that the heat of adsorption of $SO_2$ was higher in the presence of $O_2$. This result was likely due to the formation of more stable sulfate species in the presence of oxygen. Tseng et al. [41] examined the sulfur interactions with copper supported on activated carbon and proposed that $SO_2$ was oxidized in the presence of oxygen to form $SO_3$ and that sulfates were then formed on the copper sites.

### 3.3. Flow reactor experiments

The effects induced by $SO_2$ treatment on the Cu-SAPO-34 were studied in detail using a monolith sample in the flow reactor system. The activities before and after sulfation were investigated with the help of procedures described in Section 2.

#### 3.3.1. Ammonia storage and TPD

Ammonia storage capacity plays an important role in the SCR system [42]. Thus, it is important to study the adsorption–desorption behavior of the catalyst. During the adsorption period, the catalyst was exposed to 400 ppm ammonia together with 8% $O_2$ and 5% $H_2O$ in Ar at 150 °C and the outlet $NH_3$ concentration is presented in Fig. 5. During the exposure of the catalyst to ammonia, there was initially a total uptake of all ammonia, followed by a breakthrough after long exposure times because of the ammonia saturation on the catalyst surface. The results in Fig. 4 show that for the sulfated catalyst, the signal for ammonia breakthrough was about 4 min earlier than the fresh catalyst, indicating a slightly smaller ammonia storage after $SO_2$ treatment. After the adsorption period, the catalyst was exposed to Ar alone; hence, the loosely bound ammonia was released. The temperature was then ramped up with 10 °C $min^{-1}$ to 500 °C, producing a desorption peak of strongly bound ammonia, with the maxima at around 354 °C. As expected, the desorption peak after the catalyst had undergone sulfur treatment ($SO_2$-1I and $SO_2$-2I) was somewhat lower than for the fresh catalyst owing to the decreasing ammonia stored during the adsorption period. However, the temperature of the maximum ammonia desorption was not significantly changed because of the sulfation. The results revealed that the sites for strongly bound ammonia were only to a very small extent affected by sulfur treatment. According to the ICP-AES results, 0.13 mmol S/(g washcoat) were present in the catalyst compared to the ammonia release of 1.49 mmol/(g washcoat) after the second sulfation. Thus, the amount of sulfur in the sample after repeated experiments was significantly less than the ammonia storage, which results in that the ammonia adsorption is influenced only to a minor extent.

#### 3.3.2. NO oxidation

Several studies [6,43,44] suggest that NO oxidation to $NO_2$ is the rate-determining step for standard SCR over zeolite-based catalysts. However, both Nedyalkova et al. [45] and Metkar et al. [44] observed that the presence of water significantly decreased the NO oxidation, but the SCR activity was only affected to a small degree [45]. Therefore, it is not likely that the rate-determining step for SCR is the NO oxidation. Even though NO oxidation is probably not rate determining, it is very interesting to examine from a mechanistic point of view. We have been studying the NO oxidation from 150 to 500 °C in the presence of 400 ppm NO, 8% $O_2$ and 5% $H_2O$. The resulting $NO_2$ concentration before and after $SO_2$ treatment is shown in Fig. 6. Although the maximum concentration reached at 500 °C was only about 6 ppm, the Cu-SAPO-34 catalyst showed an NO oxidation activity that increased with increasing temperature. At high temperature, $NO_2$ production usually decreases due to thermodynamic restriction [43]; the reason why this was not observed in our study was the low activity for NO oxidation, resulting in the fact that the $NO_2$ level was far from the thermodynamic level. In a recent study by Kwak et al. [46], the NO oxidation over Cu-SSZ-13 with different copper loadings was examined. They further observed that despite the high $NO_x$ conversion during SCR, there was low oxidation activity of the catalysts; hence, NO oxidation might not be the crucial step for NO reduction over Cu-SSZ-13, an observation consistent with those made by Nedyalkova et al. [45]. In addition, Metkar et al. [47] discovered the lower oxidation activity of Cu-CHA compared to Fe-ZSM5-5 and argued that the NO oxidation was inhibited because of the more stably adsorbed $NO_2$ to form more surface nitrates on Cu-CHA than on Fe-ZSM-5. Mihai et al. [48] observed that while the NO oxidation rate was lower for under-exchanged Cu samples for Cu-BEA, it increased with the copper exchange level. In our previous study [48], we proposed that NO oxidation predominantly took place on the over-exchanged sites. These results are consistent with the present result, where we observe a low NO oxidation over Cu-SAPO-34 at the same time as the catalyst has a low ion-exchanged level (0.12 Cu/Si ratio).

After the catalyst underwent sulfur treatment, the NO oxidation activities ($SO_2$-1G and $SO_2$-2G) were only slightly suppressed at high temperatures. Thus, the copper sites responsible for NO

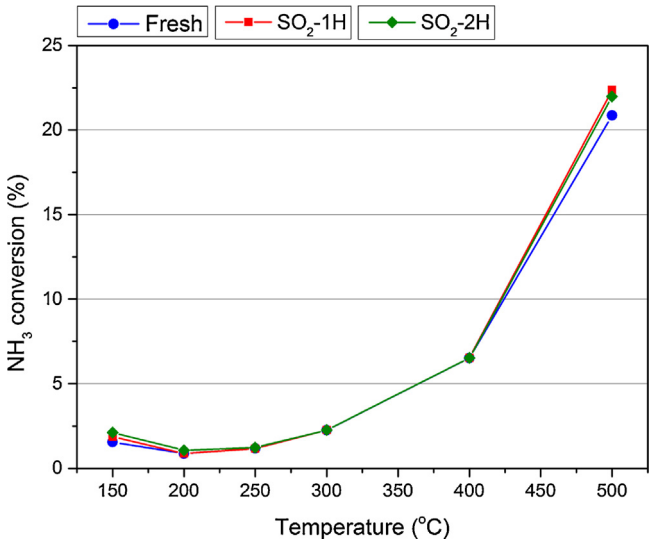


**Fig. 7.** Steady-state $NH_3$ conversion during $NH_3$ oxidation from 150 to 500 °C over fresh and sulfated Cu-SAPO-34. The catalyst was exposed to 400 ppm $NH_3$ + 8% $O_2$ and 5% $H_2O$ in Ar. The experimental notation is presented in Table 1.

oxidation seemed to be affected only to a minor extent. However, due to the low conversion, it is difficult to make a conclusive statement.

### 3.3.3. Ammonia oxidation

It is well known that at high temperature, the SCR activity declines due to the competition between ammonia oxidation and $NO_x$ reduction, which results in less ammonia being available for $NO_x$ reduction [9,43,47]. Fig. 7 presents the outlet concentration of $NH_3$ at a steady-state condition during $NH_3$ oxidation from 150 up to 500 °C for both fresh and sulfur-treated cases ($SO_2$-1H and $SO_2$-2H). It can be seen in Fig. 7 that the Cu-SAPO-34 exhibits a trend in $NH_3$ oxidation activity similar to other zeolite-based catalysts discussed in the literature [12,42,44,49]. The conversion of ammonia, although very low, starts at 300 °C and increases with higher reaction temperatures, with a maximum conversion of 21% at 500 °C for a fresh catalyst. However, in the same way as for the NO oxidation, the ammonia oxidation activity is low. These results are consistent with the study by Mihai et al. [48] showing that Cu-BEA with low copper loading possesses low activity for both reactions. During $NH_3$ oxidation over Cu-SAPO-34, negligible amounts of $NO_x$ and $N_2O$ are formed (data not shown here). Thus, almost all $NH_3$ is converted into $N_2$ according to the following reaction:

$$4NH_3 + 3O_2 \rightarrow 2N_2 + 6H_2O \quad (4)$$

After the first and second sulfur exposures, the ammonia oxidation activity of the samples, $SO_2$-1H and $SO_2$-2H, respectively, remains stable indicating that the metal sites responsible for ammonia oxidation were not significantly affected by the sulfur poisoning, which was also the case with NO oxidation.

### 3.3.4. Standard SCR

In the case where $NO_x$ source is exclusively NO, $NO_x$ reduction would follow the so-called standard SCR reaction, as mentioned earlier (see Eq. (1)). Fig. 8 displays the steady-state concentrations as a function of reaction temperature for $NH_3$ (A), $NO_x$ (B) and $N_2O$ (C) in the outlet stream of the reactor during the standard SCR reaction over Cu-SAPO-34 when the temperature is stepwise increased from 150 to 500 °C. In addition, the impact of sulfur deactivation of the catalyst is presented by Fig. 8, where the experimental notation was given in Table 1. The fresh Cu-SAPO-34 catalyst showed results consistent with the standard SCR reaction, consuming an approximately similar amount of $NH_3$ and NO [50]. The NO conversion was increased when increasing the temperature up to 400 °C, where the $NO_x$ reduction reached 89% for the fresh catalyst. When the temperatures further increased, the conversion declined because of the increased ammonia oxidation activity. However, the decrease in conversion at 500 °C was only minor due to the low activity for the ammonia oxidation over this catalyst (see Fig. 7).

After the first sulfur treatment, the standard SCR experiments were repeated five times in order to achieve stable activity. As seen in Fig. 8B, the activity of the catalyst after sulfation was initially significantly decreased ($SO_2$-1A) after which the activity gradually recovered by repeating the standard SCR: $SO_2$-1B (results not shown here), $SO_2$-1C, $SO_2$-1D and $SO_2$-1E (for notation, see Table 1). This development might be attributable to desorption of the loosely

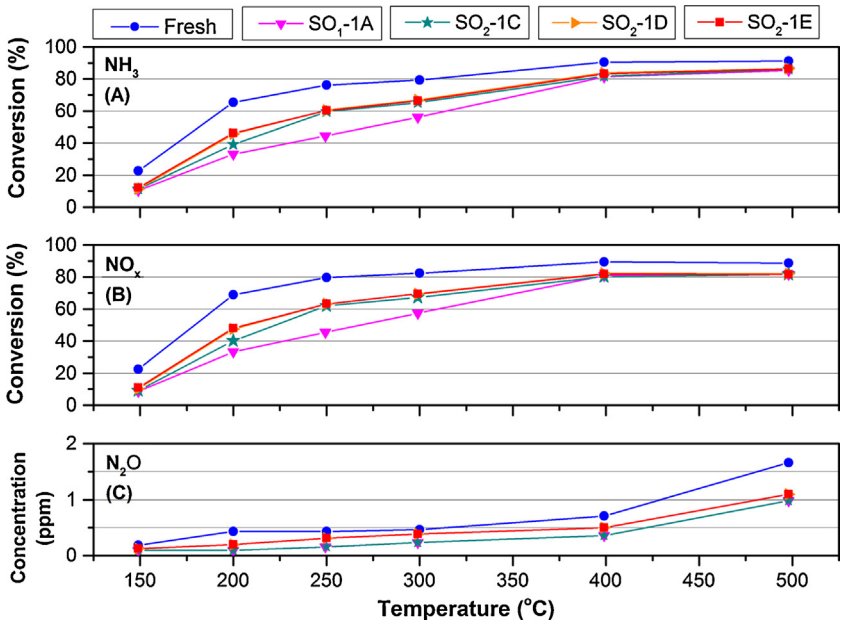


**Fig. 8.** Steady-state conversion of $NH_3$ (A), $NO_x$ (B) and concentration of $N_2O$ (C) during standard SCR reaction over fresh Cu-SAPO-34 and after the first $SO_2$ treatment. The sample was exposed to 400 ppm $NH_3$ + 400 ppm NO + 8% $O_2$ + 5% $H_2O$ in Ar. The experimental notation is presented in Table 1.

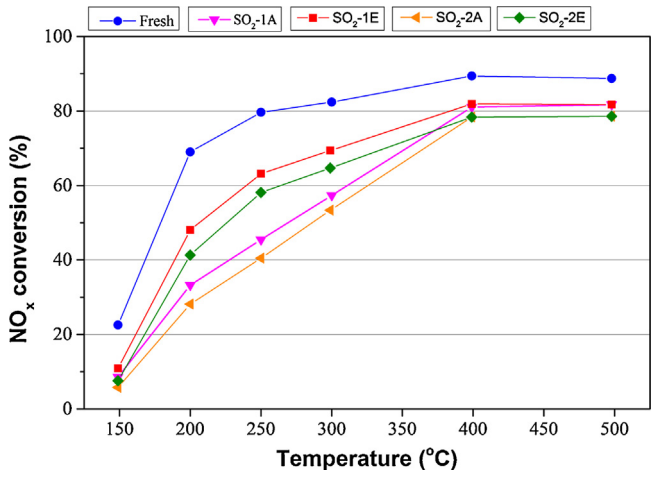


**Fig. 9.** $NO_x$ conversion versus temperature for standard SCR over Cu-SAPO-34 for fresh and sulfated catalyst. The sample was exposed to 400 ppm $NH_3$ + 400 ppm NO + 8% $O_2$ + 5% $H_2O$ in Ar. The experimental notation is presented in Table 1.

bound sulfur on the surface of the catalyst during reaction conditions at high temperature or alternatively, the sulfur might be moved to other sites on the catalyst which were not active in the SCR reaction. However, the initial activity of Cu-SAPO-34 was never regained and a substantial deactivation was observed; for example, after the first $SO_2$ treatment, the $NO_x$ conversion at 250 °C was only 63% compared to 79% for the fresh catalyst. Thus, there was still strongly bound sulfur present on the surface, which was consistent with the ICP-SFMS results previously discussed. Zhang et al. [33] who studied the impact of sulfur on commercial Cu-SAPO-34 sample showed that several factors contributed to the deactivation including formation of ammonium sulfate species, competitive adsorption between $SO_2$ and $NO_2$, and formation of metal sulfate species. Due to the different experimental procedure that we had in our case, with only $SO_2$, oxygen and water present during poisoning the copper sulfate species formation (or possibly other $SO_2$ species on the copper sites) is likely responsible for the lowering activity of $NO_x$ reduction. In addition, XPS study by Cheng et al. [30] confirmed the existence of sulfates after Cu/zeolite sample poisoned with $SO_2$.

In order to investigate the possibility that the catalyst might further deactivate, a second sulfation was performed on the same sample, following the same procedure as the first procedure. Thereafter, five standard SCR reactions were performed, denoted as $SO_2$-2A, etc. (see Table 1 for notation) with the results shown in Fig. 9. The general trends, which were observed after the catalyst had undergone its first $SO_2$ treatment, were also found after the second sulfation. Initially, there was a large deactivation ($SO_2$-2A) and some of the catalyst activity was restored progressively with standard SCR reaction steps. After five standard SCR reaction steps, the catalyst reached its stable activity, which was slightly lower than after its first $SO_2$ treatment (compare $SO_2$-1E and $SO_2$-2E in Fig. 9). To conclude, the results showed that additional sites on the catalyst were deactivated by the second sulfur treatment, although the differences are small.

In addition, referring to the previous experiments, the ammonia and NO oxidation activities were only slightly affected by the $SO_2$ treatment (see Figs. 6 and 7), while the SCR functions deactivated significantly (see Figs. 8 and 9). Mihai et al. [48] examined these reactions over Cu-BEA and observed that the rate for NO and ammonia oxidation was higher for over-exchanged sites, whereas for the SCR reaction, opposite results were obtained. Xue et al. [36] examined the effect of Cu loading on the SCR reaction rate for Cu-SAPO-34 and observed that medium-loaded samples showed a higher SCR activity than high-loaded Cu-SAPO-34, even though the lowest loading also showed a lower activity than medium-loaded samples. Xue et al. [36] proposed that there are different Cu sites in Cu-SAPO-34 and that only some of them are responsible for the SCR activity. We therefore suggest that for Cu-SAPO-34, in the same way as for Cu-BEA, the NO and ammonia oxidation occurs on one type of site, possibly predominating in over-exchanged samples, while the SCR reaction occurs on another Cu site. Based on our results, we suggest that the sites responsible for the SCR reaction are more significantly poisoned by sulfur than the sites where the oxidation reactions occur.

Selectivity towards $N_2O$ production is one of the main aspects of the $NH_3$-SCR system. As seen in Fig. 8C, Cu-SAPO-34 only produced a maximum of less than 2 ppm $N_2O$ during the standard SCR reaction. In general, catalysts with CHA structure like Cu-SAPO-34 and Cu-SSZ-13 offer an excellent selectivity of $NO_x$ reduction due to small amount of $N_2O$ production compared to other zeolite catalysts such as Cu-BEA [51] and Cu-ZSM-5 [10]. Further, Ma et al. [22] who investigated the activity of both Cu-SAPO-34 and Cu-SSZ-34 with similar Cu content observed that Cu-SAPO-34 produced significantly less $N_2O$ especially at high temperature. It is worth to note that for catalysts with low copper loading less $N_2O$ is formed during the reaction [21,51].

### 3.3.5. SCR with $NO_2/NO_x = 0.5$

The rate of $NO_x$ reduction can be greatly enhanced with the presence of $NO_2$ in the feed with a ratio of $NO_2/NO_x = 0.5$ which follows the so-called fast SCR [51]. This reaction was studied using 400 ppm $NH_3$, together with an equimolar amount of NO and $NO_2$ (200 ppm) in the presence of 8% $O_2$ and 5% $H_2O$; the result is presented in Fig. 10.

Initially, when the catalyst is exposed to the gas mixture at 150 °C, the total uptake of ammonia (Fig. 10A) was observed while the $NO_x$ conversion (Fig. 10B) is simultaneously increasing. The reason is that the reaction rate for the fast SCR is depending on the ammonia coverage on the surface; when the coverage is increasing over time, the SCR rate is increasing. However, the $NO_x$ concentration exhibits a minimum after which it starts again to increase probably because of the formation of ammonium nitrates that block the active site for the SCR reaction [52,53], hence hindering the reduction of $NO_x$ as seen in Fig. 10B. Ammonium nitrate can be formed through the following reaction [5,54]:

$$2NH_3 + 2NO_2 \rightarrow NH_4NO_3 + N_2 + H_2O \quad (5)$$

but it should be mentioned that depending on the conditions [48], ammonium nitrate might form different species and complexes. The formation of ammonium nitrate types of species occurs predominately through reactions with $NO_2$ consistent with the fact that the $NO_2$ consumption at low temperatures is significantly higher than NO (see Fig. 11).

At higher temperature, ammonium nitrates on the surface start to decompose following the reaction [5,21,54]:

$$NH_4NO_3 \rightarrow N_2O + 2H_2O \quad (6)$$

An increase in $N_2O$ production, from less than 1 ppm at 200 °C to 5 ppm at 250 °C was observed. Simultaneously, the $NO_x$ conversion was steadily increasing (Fig. 10B). The reason for this gradual improvement is probably the decomposition of ammonium nitrates that blocked the active SCR sites. Further, when the temperature was ramped from 250 to 300 °C, a substantial peak in $N_2O$ was observed (Fig. 10B) because of the removal of the ammonium nitrate species. At 300 °C, because the activity was exceedingly high, the majority of these species was likely removed. Interestingly, this blocking effect was only minor for Cu-BEA with 50% $NO_2$ (data not shown here). Thus, ammonium nitrate formation seemed to occur more easily on Cu-SAPO-34 than on Cu-BEA, at least with

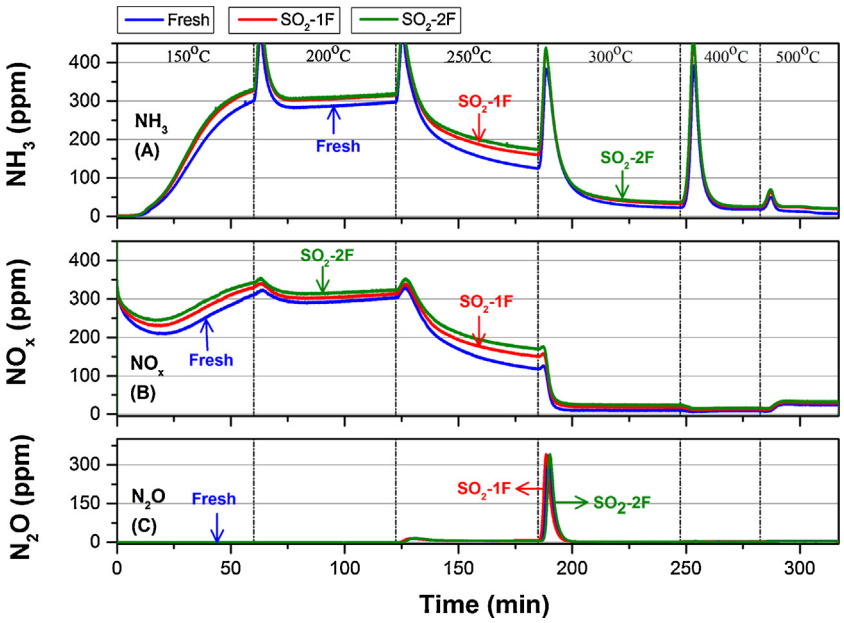


**Fig. 10.** Concentration of $NH_3$ (A), $NO_x$ (B) and $N_2O$ (C) as a function of time during fast SCR over fresh and sulfated Cu-SAPO-34. The catalyst was exposed to 400 ppm $NH_3$ + 200 pm NO + 200 ppm $NO_2$ + 8% $O_2$ + 5% $H_2O$ in Ar. The experimental notation is presented in Table 1.

a 50% $NO_2$ to $NO_x$ ratio. For Cu-SAPO-34, the standard SCR possessed a higher activity than the fast SCR at low temperature due to the ammonium nitrate blocking, which was not the case for Cu-BEA [51] and Cu-ZSM-5 [10]. However, at high temperatures, due to the removal of ammonium nitrates blocking the sites, the fast SCR predominantly occurred which resulted in a higher conversion of $NO_x$ compared to the standard SCR. The fresh catalyst exhibited a $NO_x$ conversion of 98% under the fast SCR conditions at 400 °C, while for standard SCR conditions the conversion was 89%. At higher temperatures, the conversion declined (Fig. 10B) because of more pronounced ammonia oxidation (Fig. 7).

Based on the results shown in Fig. 10, at temperatures up to 250 °C, there was an observed impact on the fast SCR reaction after the catalyst had been sulfated. For example at 250 °C, the $NO_x$ conversion decreased from 70% for fresh conditions to 61 ($SO_2$-1F) and 57% ($SO_2$-2F) after it had undergone first and second $SO_2$ treatments, respectively. However, at higher temperatures (300–500 °C), this effect was hardly detectable, e.g. the sulfated catalyst showed a maximum decrease of only 2% compared to the fresh condition. It should be noted that at high temperatures, there was close to full conversion and it was therefore difficult to determine the deactivation. To conclude, the standard SCR reaction was more affected by sulfur treatment than the fast SCR. For example, at 250 °C, the conversion at the end of the step was decreasing due to sulfur poisoning from 79% to 57% ($SO_2$-2E) for the standard SCR, while it was only decreasing from 70% to 57% ($SO_2$-2F) for the fast SCR. This result was in good agreement with the finding of Schmieg and Lee [24], who suggested that the impact of sulfur poisoning on Cu-zeolite catalysts can be minimized if the composition of $NO_2/NO_x$ can be adjusted to 50%.

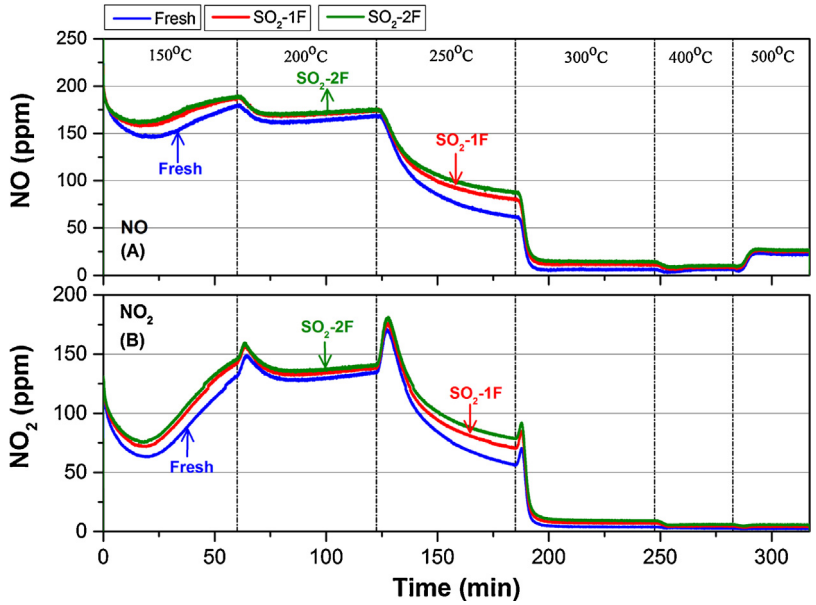


**Fig. 11.** Concentration of NO (A) and $NO_2$ (B) during the fast SCR over fresh and sulfated Cu-SAPO-34. The catalyst was exposed to 400 ppm $NH_3$ + 200 ppm NO + 200 ppm $NO_2$ + 8% $O_2$ + 5% $H_2O$ in Ar. The experimental notation is presented by Table 1.

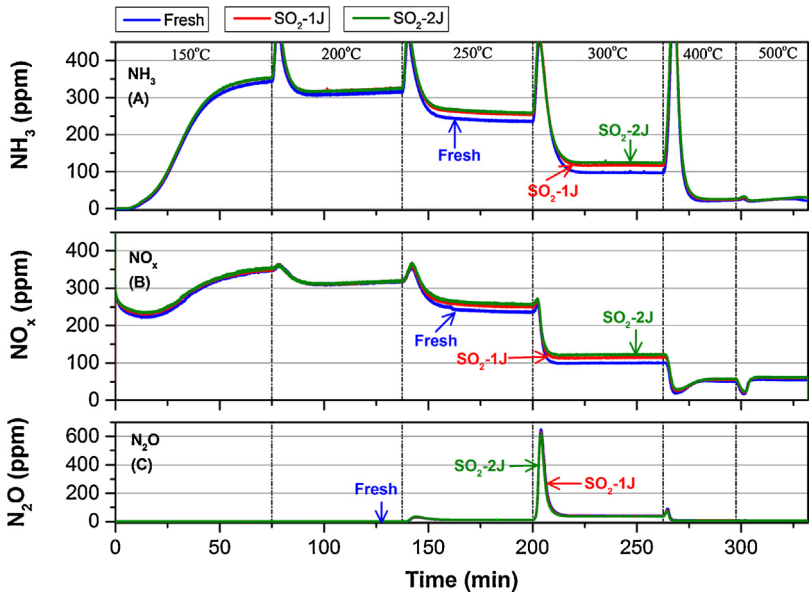


**Fig. 12.** Outlet concentration of $NH_3$ (A), $NO_x$ (B) and $N_2O$ (C) during the SCR with $NO_2/NO_x$ = 75% over fresh and sulfated Cu-SAPO-34. The catalyst was exposed to 400 ppm $NH_3$ + 100 ppm NO + 300 ppm $NO_2$ + 8% $O_2$ + 5% $H_2O$ in Ar. The experimental notation is presented in Table 1.

In the standard SCR, the reaction proceeds via a redox mechanism between $Cu^+$ and $Cu^{2+}$ [21,55] and the equimolar NO and $NO_2$ in the feed has been regarded as the optimal condition to obtain high conversion in $NO_x$ reduction [6,54,56]. Even though the mechanism of the fast SCR in Cu-CHA catalysts has not been well understood, the metal cation is still believed to play an important role [21]. According to our results for the standard SCR experiments, the copper sites were deactivated due to the sulfur treatment, whereas with already available $NO_2$ in the feed, the fast SCR reaction was less sensitive to the $SO_2$ treatment. These results indicate that the standard and fast SCR reactions proceed on different sites or using different mechanisms.

Unlike other zeolite-based catalysts, e.g. Cu-ZSM-5 [10] and Cu-BEA [51], the Cu-SAPO-34 showed a low $N_2O$ production under fast SCR conditions, with a maximum of only about 6 ppm as presented by Fig. 10C. The yield of $N_2O$ for the fast SCR was higher than during the standard SCR, which demonstrates a correlation between the amount of $NO_2$ in the feed and the $N_2O$ production, which is in agreement with previous investigations [57].

### 3.3.6. SCR with $NO_2/NO_x$ = 0.75

Due to the importance of $NO_2$ presence for the conversion of $NO_x$, it is interesting to study the $NH_3$-SCR reaction with high ratios of $NO_2$ to $NO_x$. Results of the experiments over fresh and sulfur-treated Cu-SAPO-34 with a feed composition of $NO_2/NO_x$ = 0.75 are depicted in Fig. 12. Trends similar to the fast SCR were observed also for this higher $NO_2$ to $NO_x$ ratio. Initially, when exposing the catalyst to the gas mixture at 150 °C, an ammonium nitrate production was observed as the $NO_x$ concentration reached a minimum after which the concentration started to increase (Fig. 12B). The ammonium nitrate species were thermally decomposed when increasing the temperature from 250 to 300 °C, resulting in a large production of $N_2O$ (Fig. 12C). For the fast SCR reaction, the ammonium nitrates started to decompose at 250 °C, causing gradually increased conversion. However, for the case of 75% $NO_2$, there was a small amount of $N_2O$ formed at 250 °C and the impact on the $NO_x$ conversion was minor. Thus, the presence of large amounts of NO destabilized the ammonium nitrates and decomposed them at lower temperature, which was observed earlier [58].

Surprisingly, the $NO_x$ conversion for the fresh catalyst with the $NO_2/NO_x$ ratio of 0.75 was somewhat lower than for the standard SCR case at high temperature. The maximum conversion for the fresh catalyst was 87%, obtained at 400 °C for an $NO_2/NO_x$ ratio of 0.75, while for the standard SCR, the conversion reached 89%. Metkar et al. [56] found similar results for the Cu-CHA catalyst, where the $NO_x$ conversion was lower for the $NO_2/NO_x$ fraction higher than 0.5 than the SCR with NO alone. A different trend was identified for the Fe-ZSM-5 catalyst, where the $NO_x$ conversion was higher for $NO_2/NO_x$ fraction larger than 0.5 compared to the NO only case although not as high as for the fast SCR. Moreover, Metkar et al. [56] concluded that for the Cu-CHA catalyst, the enhancement of $NO_x$ activity due to the $NO_2$ addition was not as significant as for the Fe-ZSM-5 catalyst. In the same way as for the standard and fast SCR, the conversion of $NO_x$ over Cu-SAPO-34, for the case with high $NO_2/NO_x$ ratio, was decreased at high temperature due to a competition with the ammonia oxidation reaction. Another feature of the $NH_3$-SCR reaction with its high fraction of $NO_2$ was that the amount of $N_2O$ was significantly higher so that the $N_2O$ maximum was more than 40 ppm higher than for the standard SCR conditions.

The SCR reaction with $NO_2/NO_x$ = 0.75 before and after sulfation of the catalyst are also presented in Fig. 12 and only minor changes in activity were observed. The $NO_x$ conversion was only decreased by 4 and 6% compared to the fresh activity after the first and second $SO_2$ treatments, respectively. Again, these results revealed that the presence of $NO_2$ resulted in less impact of the sulfur poisoning compared to standard SCR. For this case ($NO_2/NO_x$ = 0.75), the effect of sulfur was even lower compared to the case with $NO_2/NO_x$ = 0.5. Our results are in line with the study by Schmieg and Lee [24], who observed less effect of the poisoning in the presence of 50% $NO_2$. These results suggested that the different SCR reactions occur on different sites and that the mechanisms seemed to be different.

## 4. Conclusions

In this study, the impact of sulfur poisoning of Cu-SAPO-34 on various reactions in the SCR mechanism has been examined. Further, a detailed characterization of the fresh and sulfur poisoned samples was conducted.

XRD results showed that the SAPO-34 structure remained after the copper had been ion-exchanged. In addition, the BET surface area and pore volume were high. Micro-calorimetry measurements of ammonia were conducted at different temperatures with results

showing that the heat of adsorption was increasing with increasing adsorption temperature from 100 to 300 °C. The reason was that at a lower temperature, more loosely bound ammonia was also adsorbed on the surface, which lowered the heat of adsorption. Surprisingly, the $\Delta H$ was similar at 400, 350 and 300 °C and a possible reason might be that when ammonia feed was shut of more than 50% of the stored ammonia was desorbed, resulting in that significant amounts of the ammonia that were adsorbed at 400 °C desorbed ad readsorbed at 350 °C, and in a similar way large amounts of the stored ammonia at 350 °C was readsorbed at 300 °C.

Sulfur treatment resulted in a lowering of the BET surface area, as well as simultaneously the pore volume because some pores were blocked. Ammonia TPD experiments showed that the storage and release of ammonia on the sulfur-poisoned sample were only slightly lower compared to the fresh catalyst. These results implied that since ammonia adsorption on acid sites was very large, only minor amounts of sulfur were attached to the acid sites. In addition, the binding strength of $SO_2$ was detected and it was observed that the heat of adsorption was high, showing that sulfur binds strongly to the catalyst sites. This result agrees well with ICP-SFMS, which showed that sulfur still remained on the catalyst after repeated experiments to 500 °C. Since the ammonia storage was only to a minor extent influenced by sulfur, it was likely that the sulfur predominantly attached to the copper sites. These results were further supported by $H_2$-TPR data, where it was clear that there was less copper available in the poisoned sample that could undergo a redox cycle. In addition, it was found that the heat of adsorption was higher when oxygen was added during the poisoning.

After the $SO_2 + O_2 + H_2O$ exposure of the catalyst at 300 °C, the standard SCR reaction was repeated five times from 150 to 500 °C. The catalyst was severely aged after the sulfur poisoning, but some of the activity was gradually gained back after repeated SCR experiments. However, in the last SCR experiments, stable conversion was reached and the activity was still significantly lower than for the fresh sample. Interestingly, although the sulfur poisoning showed a large effect on the SCR activity, there was only a minor effect on the ammonia and NO oxidation. The activity for NO and ammonia oxidation was also low on this sample. In an earlier study, we proposed that over Cu/BEA, ammonia and NO oxidation would predominantly occur over over-exchanged copper sites, while SCR was faster on the low- and medium-loaded Cu-BEA. Based on the results of the present study, we propose that this is also the case for Cu-SAPO-34 and since the current catalyst has a low ion-exchange level, this is the reason for the low ammonia and NO oxidation.

A second sulfur poisoning was conducted on the same monolith resulting in a similar trend, with higher initial deactivation followed by a gradual increase of activity after repeated SCR experiments. After a few SCR experiments, a stable SCR activity was gained, which was lower than after the first sulfur exposure. Interestingly, the sulfur poisoning had a lower impact on the fast SCR and even a smaller effect on the $NO_2$ SCR reactions compared to the standard SCR, implying that the reactions occurred on different sites in the presence of $NO_2$ or that the mechanism was different. Another interesting feature with the results for the fast SCR was that large amounts of ammonium nitrate species were likely formed at lower temperatures, thereby blocking the copper sites and reducing the activity. When further increasing the temperature, a large $N_2O$ release peak was observed due to ammonium nitrate decomposition, after which high activity was witnessed. The Cu-SAPO-34 showed substantially more blocking of ammonium nitrates than could be seen in our earlier studies of Cu-ZSM-5 and Cu-BEA.

## Acknowledgements

This study was performed at Chemical Engineering and Competence Centre for Catalysis, Chalmers University and Cummins Inc. The financial support of Cummins Inc., the Swedish Foundation for Strategic Research (F06-0006) and the Swedish Research Council (621-2011-4860) are gratefully acknowledged.

## References

[1] E.E. Agency, Air Quality in Europe—2013 Report, European Environment Agency, Copenhagen, 2013.
[2] P. Forzatti, Applied Catalysis A: General 222 (2001) 221–236.
[3] M.V. Twigg, Catalysis Today 163 (2011) 33–41.
[4] G. Busca, L. Lietti, G. Ramis, F. Berti, Applied Catalysis B: Environmental 18 (1998) 1–36.
[5] M. Koebel, G. Madia, M. Elsener, Catalysis Today 73 (2002) 239–247.
[6] M. Devadas, O. Kröcher, M. Elsener, A. Wokaun, N. Söger, M. Pfeifer, Y. Demel, L. Mussmann, Applied Catalysis B: Environmental 67 (2006) 187–196.
[7] S. Brandenberger, O. Kröcher, A. Tissler, R. Althoff, Catalysis Reviews 50 (2008) 492–531.
[8] K. Rahkamaa-Tolonen, T. Maunula, M. Lomma, M. Huuhtanen, R.L. Keiski, Catalysis Today 100 (2005) 217–222.
[9] O. Kröcher, M. Devadas, M. Elsener, A. Wokaun, N. Söger, M. Pfeifer, Y. Demel, L. Mussmann, Applied Catalysis B: Environmental 66 (2006) 208–216.
[10] H. Sjövall, L. Olsson, E. Fridell, R.J. Blint, Applied Catalysis B: Environmental 64 (2006) 180–188.
[11] K. Kamasamudram, N. Currier, T. Szailer, A. Yezerets, SAE International Journal of Fuels and Lubricants 3 (2010) 664–672.
[12] N. Wilken, K. Wijayanti, K. Kamasamudram, N.W. Currier, R. Vedaiyan, A. Yezerets, L. Olsson, Applied Catalysis B: Environmental 111–112 (2012) 58–66.
[13] S. Shwan, R. Nedyalkova, J. Jansson, J. Korsgren, L. Olsson, M. Skoglundh, Industrial & Engineering Chemistry Research 51 (2012) 12762–12772.
[14] J.H. Park, H.J. Park, J.H. Baik, I.S. Nam, C.H. Shin, J.H. Lee, B.K. Cho, S.H. Oh, Journal of Catalysis 240 (2006) 47–57.
[15] S. Brandenberger, O. Kröcher, M. Casapu, A. Tissler, R. Althoff, Applied Catalysis B: Environmental 101 (2011) 649–659.
[16] J. Luo, A. Yezerets, C. Henry, H. Hess, K. Kamasamudram, H.-Y. Chen, W.S. Epling, Hydrocarbon Poisoning of Cu-Zeolite SCR Catalysts, SAE Technical Paper 2012-01-1096, 2012, http://dx.doi.org/10.4271/2012-01-1096.
[17] C. Montreuil, C. Lambert, SAE International Journal of Fuels and Lubricants 1 (2008) 495–504.
[18] R.G. Silver, M.O. Stefanick, B.I. Todd, Catalysis Today 136 (2008) 28–33.
[19] P. Kern, M. Klimczak, T. Heinzelmann, M. Lucas, P. Claus, Applied Catalysis B: Environmental 95 (2010) 48–56.
[20] D.W. Fickel, E. D'Addio, J.A. Lauterbach, R.F. Lobo, Applied Catalysis B: Environmental 102 (2011) 441–448.
[21] F. Gao, J. Kwak, J. Szanyi, C.F. Peden, Topics in Catalysis 56 (2013) 1441–1459.
[22] L. Ma, Y. Cheng, G. Cavataio, R.W. McCabe, L. Fu, J. Li, Chemical Engineering Journal 225 (2013) 323–330.
[23] M. Moliner, C. Franch, E. Palomares, M. Grill, A. Corma, Chemical Communications 48 (2012) 8264–8266.
[24] S.J. Schmieg, J. Lee, Evaluation of Supplier Catalyst Formulations for the Selective Catalytic Reduction of $NO_x$ With Ammonia, SAE Technical Paper 2005-01-3881, 2005, http://dx.doi.org/10.4271/2005-01-3881.
[25] G. Cavataio, J. Girard, J.E. Patterson, C. Montreuil, Y. Cheng, C.K. Lambert, Laboratory Testing of Urea-SCR Formulations to Meet Tier 2 Bin 5 Emissions, SAE Technical Paper 2007-01-1575, 2007, http://dx.doi.org/10.4271/2007-01-1575.
[26] Y. Cheng, C. Montreuil, G. Cavataio, C. Lambert, SAE International Journal of Fuels and Lubricants 1 (2008) 471–476.
[27] J.W. Girard, C. Montreuil, J. Kim, G. Cavataio, C. Lambert, SAE International Journal of Fuels and Lubricants 1 (2008) 488–494.
[28] J.A. Ura, J. Girard, G. Cavataio, C. Montreuil, C. Lambert, Cold Start Performance and Enhanced Thermal Durability of Vanadium SCR Catalysts, SAE Technical Paper 2009-01-0625, 2009, http://dx.doi.org/10.4271/2009-01-0625.
[29] Y. Cheng, C. Montreuil, G. Cavataio, C. Lambert, The Effects of $SO_2$ and $SO_3$ Poisoning on Cu/Zeolite SCR Catalysts, SAE Technical Paper 2009-01-0898, 2009, http://dx.doi.org/10.4271/2009-01-0898.
[30] Y. Cheng, C. Lambert, D.H. Kim, J.H. Kwak, S.J. Cho, C.H.F. Peden, Catalysis Today 151 (2010) 266–270.
[31] M. Castagnola, J. Caserta, S. Chatterjee, H. Chen, R. Conway, J. Fedeyko, W. Klink, P. Markatou, S. Shah, A. Walker, Engine Performance of Cu- and Fe-Based SCR Emission Control Systems for Heavy Duty Diesel Applications, SAE Technical Paper 2011-01-1329, 2011, http://dx.doi.org/10.4271/2011-01-1329.
[32] A. Kumar, M.A. Smith, K. Kamasamudram, N.W. Currier, H. An, A. Yezerets, Catalysis Today 231 (2014) 75.
[33] L. Zhang, D. Wang, Y. Liu, K. Kamasamudram, J. Li, W. Epling, Applied Catalysis B: Environmental 156–157 (2014) 371–377.
[34] A.M. Prakash, S. Unnikrishnan, Journal of the Chemical Society, Faraday Transactions 90 (1994) 2291.
[35] K. Leistner, L. Olsson, Applied Catalysis B: Environmental 165 (2015) 192–199.
[36] J. Xue, X. Wang, G. Qi, J. Wang, M. Shen, W. Li, Journal of Catalysis 297 (2013) 56–64.

[37] F. Gao, E.D. Walter, N.M. Washton, J. Szanyi, C.H.F. Peden, ACS Catalysis 3 (2013) 2083–2093.
[38] N. Wilken, K. Kamasamudram, N.W. Currier, J. Li, A. Yezerets, L. Olsson, Catalysis Today 151 (2010) 237–243.
[39] G. Boskovic, T. Vulic, E. Kis, P. Putanov, Chemical Engineering & Technology 24 (2001) 269–274.
[40] S.P. Felix, C. Savill-Jowitt, D.R. Brown, Thermochimica Acta 433 (2005) 59–65.
[41] H.-H. Tseng, M.-Y. Wey, Carbon 42 (2004) 2269–2278.
[42] H. Sjövall, R.J. Blint, L. Olsson, The Journal of Physical Chemistry C 113 (2009) 1393–1405.
[43] L. Olsson, H. Sjövall, R.J. Blint, Applied Catalysis B: Environmental 87 (2009) 200–210.
[44] P.S. Metkar, N. Salazar, R. Muncrief, V. Balakotaiah, M.P. Harold, Applied Catalysis B: Environmental 104 (2011) 110–126.
[45] R. Nedyalkova, K. Kamasamudram, N.W. Currier, J. Li, A. Yezerets, L. Olsson, Journal of Catalysis 299 (2013) 101–108.
[46] J. Kwak, D. Tran, J. Szanyi, C.F. Peden, J. Lee, Catalysis Letters 142 (2012) 295–301.
[47] P.S. Metkar, V. Balakotaiah, M.P. Harold, Catalysis Today 184 (2012) 115–128.
[48] O. Mihai, C.R. Widyastuti, S. Andonova, K. Kamasamudram, J. Li, S.Y. Joshi, N.W. Currier, A. Yezerets, L. Olsson, Journal of Catalysis 311 (2014) 170–181.
[49] S. Shwan, J. Jansson, J. Korsgren, L. Olsson, M. Skoglundh, Catalysis Today 197 (2012) 24–37.
[50] L. Olsson, H. Sjövall, R.J. Blint, Applied Catalysis B: Environmental 81 (2008) 203–217.
[51] O. Mihai, C. Widyastuti, A. Kumar, J. Li, S. Joshi, K. Kamasamudram, N. Currier, A. Yezerets, L. Olsson, Catalysis Letters 144 (2014) 70–80.
[52] A. Grossale, I. Nova, E. Tronconi, D. Chatterjee, M. Weibel, Journal of Catalysis 256 (2008) 312–322.
[53] I. Malpartida, O. Marie, P. Bazin, M. Daturi, X. Jeandel, Applied Catalysis B: Environmental 113–114 (2012) 52–60.
[54] C. Ciardelli, I. Nova, E. Tronconi, D. Chatterjee, B. Bandl-Konrad, M. Weibel, B. Krutzsch, Applied Catalysis B: Environmental 70 (2007) 80–90.
[55] D. Wang, L. Zhang, J. Li, K. Kamasamudram, W.S. Epling, Catalysis Today 231 (2014) 64–74.
[56] P.S. Metkar, M.P. Harold, V. Balakotaiah, Chemical Engineering Science 87 (2013) 51–66.
[57] J.H. Kwak, D. Tran, S.D. Burton, J. Szanyi, J.H. Lee, C.H.F. Peden, Journal of Catalysis 287 (2012) 203–209.
[58] M. Colombo, I. Nova, E. Tronconi, Catalysis Today 197 (2012) 243–255.